

# IGNIS: A Robust Neural Network Framework for Constrained Parameter Estimation in Archimedean Copulas

Agnideep Aich<sup>1\*</sup>, Ashit Baran Aich<sup>2</sup> and Bruce Wade<sup>3</sup>

<sup>1</sup> Department of Mathematics, University of Louisiana at Lafayette,  
Lafayette, Louisiana, USA.

<sup>2</sup> Department of Statistics, formerly of Presidency College,  
Kolkata, India.

<sup>3</sup> Department of Mathematics, University of Louisiana at Lafayette,  
Lafayette, Louisiana, USA.

## Abstract

We introduce **IGNIS**, a deep-learning framework for *constrained* parameter estimation in Archimedean copulas with natural domain  $\theta \geq 1$ . While illustrated here on four families (Gumbel, Joe, and the novel A1/A2 copulas), IGNIS is readily applicable to any one-parameter Archimedean model with  $\theta \geq 1$ . Classical estimators (Method of Moments (MoM), Maximum Likelihood Estimation (MLE), Maximum Pseudo-Likelihood (MPL)) break down on A1/A2 due to non-monotonic dependence mappings, steep likelihood gradients, and the need for custom constraint handling. IGNIS sidesteps these issues by learning a direct mapping from four summary statistics (Kendall’s  $\tau$ , Spearman’s  $\rho$ , empirical 0.95 tail-dependence, Pearson  $r$ ) plus a one-hot family indicator to  $\theta$ , ending in a softplus + 1 output layer that *automatically enforces*  $\hat{\theta} \geq 1$ . Trained on 500 simulated  $\theta$  values per family (10 000 observations each), IGNIS outperforms MoM in extensive simulations and delivers accurate, stable estimates on real-world AAPL–MSFT returns and CDC Diabetes data. Our results demonstrate a unified, constraint-aware neural estimator for modern copula-based dependence modeling, easily extendable to any copula family respecting  $\theta \geq 1$ .

**Keywords:** IGNIS Network, Archimedean Copulas, Parameter Estimation, Neural Networks, Dependency Modeling

*MSC 2020 Subject Classification:* 62H05, 62H12, 62F10, 68T07, 62-08

## 1. Introduction

Copulas have become indispensable tools in multivariate analysis, enabling researchers to model complex dependencies among random variables by separating the marginal distributions from the dependence structure. Since Sklar’s seminal work in 1959 [1] and subsequent advances by Nelsen [2], copulas have been widely applied in finance, insurance, hydrology, healthcare and environmental science.

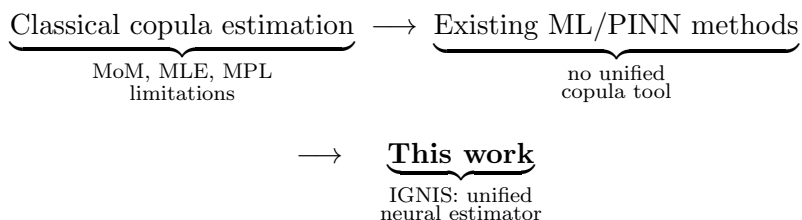
Classical parameter estimation methods for Archimedean copulas, such as the Method of Moments (MoM) [3], Maximum Likelihood Estimation (MLE), and Maximum Pseudo-Likelihood (MPL) [5], all hinge on inverting theoretical relationships (e.g. the Kendall’s  $\tau$ – $\theta$  mapping) or on optimizing highly nonlinear likelihoods. When applied to the recently proposed A1 and A2

---

\*Corresponding author: Agnideep Aich, [agnideep.aich1@louisiana.edu](mailto:agnideep.aich1@louisiana.edu), ORCID: [0000-0003-4432-1140](https://orcid.org/0000-0003-4432-1140)

families, (introduced in [6] as the A and B copulas to capture both upper and lower tail dependencies via complex generator forms) these classical approaches break down: (i) A1’s  $\tau$ - $\theta$  curve is non-monotonic, so MoM cannot recover a unique solution; (ii) A2 has high lower bound of MoM making it unsuitable for a lot of datasets (iii) both A1 and A2 generators induce extremely steep gradients in the likelihood, leading to numerical instability; and (iv) enforcing the natural constraint  $\theta \geq 1$  requires custom, constraint-aware optimizers not offered by standard packages.

Recent machine-learning and physics-informed neural network (PINN) frameworks have shown promise for data-driven parameter estimation in scientific domains ([7];[8];[9]). However, there is currently no unified neural approach that (1) handles non-monotonic dependency mappings, (2) enforces theoretical parameter constraints, and (3) generalizes across multiple Archimedean copula families. In other words:



Motivated by these gaps, we introduce the **IGNIS Framework**, a deep-learning estimator that learns a direct mapping from observable dependency statistics to the copula parameter  $\theta$ , without inverting analytic formulas. We use IGNIS to estimate parameters of four Archimedean families namely, Gumbel [10], Joe [11] and the newly developed A1/A2 copulas [6]. All these 4 copulas share the same constrained parameter domain, namely  $\theta \geq 1$ . Our main contributions are:

- 1. Unified neural architecture:** We design a multi-input network combining continuous dependency measures (Kendall’s  $\tau$ , Spearman’s  $\rho$ , empirical tail-dependence, Pearson correlation) with a one-hot copula identifier across four Archimedean families (Gumbel, Joe, A1, A2).
- 2. Theory-guided constraint enforcement:** A softplus +1 output layer automatically guarantees  $\hat{\theta} \geq 1$ , ensuring all theoretical domains are respected.
- 3. Comprehensive evaluation:** Trained on simulated datasets spanning  $\theta \in [1, 20]$ , IGNIS outperforms MoM in simulations and delivers stable estimates on real-world data (AAPL-MSFT returns, CDC Diabetes indicators).

The remainder of this paper is organized as follows. Section 2 reviews related work. Section 3 presents necessary preliminaries. Section 4 provides motivation for our work. Section 5 details the IGNIS architecture and training protocol. Section 6 presents the simulation results for IGNIS, and Section 7 demonstrates real-data applications. Finally, Section 8 concludes and outlines future research directions.

## 2. Related Work

Parameter estimation for Archimedean copulas has traditionally relied on moment-based and likelihood-based methods. The Method of Moments (MoM), leveraging Kendall’s  $\tau$  or Spearman’s  $\rho$ , has been widely adopted due to its computational simplicity ([2];[3]). However, MoM’s effectiveness hinges on the monotonicity of the  $\tau$ - $\theta$  relationship, a property absent in the novel A1 copula. Maximum Likelihood Estimation (MLE) and its pseudo-likelihood variants [5] offer alternatives but face numerical instabilities with complex density functions like those of A1/A2 copulas.

Recent advances in machine learning have introduced data-driven approaches to statistical estimation. Physics-informed neural networks introduced by Raaissi et al. in 2019 [7] and the work of Kissas et al. in 2020 [8] demonstrate how neural networks can learn complex mappings while respecting theoretical constraints. In copula modeling, Sirignano et al. in 2018 [9] pioneered neural PDE solvers for high-dimensional dependence structures, though their focus was not on parameter estimation. To our knowledge, no prior work has developed a unified neural framework for Archimedean copula parameter estimation that simultaneously addresses non-monotonicity, constraint enforcement, and multi-family compatibility, gaps our IGNIS Network fills.

### 3. Preliminaries

#### 3.1 Copulas and Dependency Modeling

Copulas are statistical tools that model dependency structures between random variables, independent of their marginal distributions. Introduced by Sklar (1959) [1], they provide a unified approach to capturing joint dependencies. Archimedean copulas, known for their simplicity and flexibility, are defined using a generator function, making them particularly effective for modeling bivariate and multivariate dependencies.

#### 3.2 The A1 and A2 Copulas

Like all Archimedean copulas, the novel A1 and A2 copulas [6] are defined through generator functions  $\phi(t)$  that are continuous, strictly decreasing, and convex on  $[0, 1]$ , with  $\phi(1) = 0$ . The A1 and A2 copulas extend the Archimedean copula framework to capture both upper and lower tail dependencies more effectively. In general, an Archimedean copula is given by:

$$C(u, v) = \phi^{-1}(\phi(u) + \phi(v)). \quad (1)$$

For the A1 copula, the generator and its inverse are defined as:

$$\phi_{A1}(t; \theta) = \left(t^{1/\theta} + t^{-1/\theta} - 2\right)^\theta, \quad \theta \geq 1, \quad (2)$$

$$\phi_{A1}^{-1}(t; \theta) = \left[ \frac{t^{1/\theta} + 2 - \sqrt{\left(t^{1/\theta} + 2\right)^2 - 4}}{2} \right]^\theta, \quad \theta \geq 1. \quad (3)$$

Similarly, for the A2 copula:

$$\phi_{A2}(t; \theta) = \left(\frac{1-t}{t}\right)^\theta (1-t)^\theta, \quad \theta \geq 1, \quad (4)$$

$$\phi_{A2}^{-1}(t; \theta) = \frac{t^{1/\theta} + 2 - \sqrt{\left(t^{1/\theta} + 2\right)^2 - 4}}{2}, \quad \theta \geq 1. \quad (5)$$

The exact formula of the Kendall's  $\tau$  for A1 and A2 copulas are given by (See Appendix A for full derivations)

$$\tau_{A1} = 1 + 2[\psi(\theta) - \psi(\theta + \frac{1}{2})], \quad (6)$$

$$\tau_{A2} = 1 - \frac{6 - 8 \ln 2}{\theta}. \quad (7)$$

Both copulas are parameterized by  $\theta \geq 1$ , which governs the strength and nature of the dependency. The dual tail-dependence structure of A1 and A2 copulas is particularly valuable for modeling extreme co-movements in joint distributions. In financial risk management, they can capture simultaneous extreme losses (lower-tail) and windfall gains (upper-tail), improving estimates of portfolio tail risk. In anomaly detection, they identify coordinated extreme events (e.g., simultaneous sensor failures in industrial systems or cyber attacks across networks) by quantifying asymmetric tail dependencies. This flexibility makes them superior to single-tailed copulas e.g., Clayton (captures only lower tails) and Gumbel (captures only upper tail) in scenarios where both tail behaviors are critical.

### 3.3 Simulation from Archimedean Copulas

In this section, we present an algorithm introduced by Genest et al. in 1993 [3] to generate an observation  $(u, v)$  from an Archimedean copula  $C$  with generator  $\phi$ .

---

**Algorithm 1** Bivariate Archimedean Copula Sampling (Genest et al., 1993)

---

**Require:** Generator  $\phi$ , its derivative  $\phi'$ , inverse  $\phi^{-1}$

**Ensure:** A single draw  $(u, v)$  from the copula

- 1: Draw  $s, t \stackrel{\text{iid}}{\sim} \text{Uniform}(0, 1)$
- 2: Define

$$K(x) = x - \frac{\phi(x)}{\phi'(x)}, \quad K^{-1}(y) = \sup\{x \mid K(x) \leq y\}$$

- 3: Compute  $w \leftarrow K^{-1}(t)$
- 4: Compute

$$u \leftarrow \phi^{-1}(s\phi(w)), \quad v \leftarrow \phi^{-1}((1-s)\phi(w))$$

- 5: **return**  $(u, v)$
- 

The above algorithm is a consequence of the fact that if  $U$  and  $V$  are uniform random variables with an Archimedean copula  $C$ , then  $W = C(U, V)$  and  $S = \frac{\phi(U)}{\phi(U)+\phi(V)}$  are independent,  $S$  is uniform  $(0, 1)$ , and the distribution function of  $W$  is  $K$ .

### 3.4 Method of Moments Estimation

The Method of Moments (MoM) is a classical statistical technique for parameter estimation, where theoretical moments of a distribution are equated with their empirical counterparts. In the context of copula modeling, MoM is particularly advantageous when direct likelihood-based estimation is challenging due to the complexity of deriving tractable probability density functions.

In this work, we derive exact analytical formulas for Kendall's  $\tau$  for both A1 and A2 copulas (see Appendix A). These formulas establish a direct relationship between Kendall's  $\tau$  and the copula parameter  $\theta$ , allowing for robust parameter estimation. By inverting this relationship, we develop MoM estimators for  $\theta$ , providing a practical approach for modeling dependencies in scenarios where traditional methods like MLE and MPL may be ineffective. However, in Section 4.2, we see that for especially A1 and even for A2, MoM is not the most efficient estimator.

## 4. Motivation

### 4.1 Limitations in Parameter Estimation Using Method of Moments

In this section, we present the results of a simulation study to estimate the parameter  $\theta$  for the A1 and A2 copulas using the **Method of Moments (MoM)**. The simulation is conducted using the **algorithm** as described in Section 3.3.

### 4.2 Results for MoM

#### Simulation Setup

- 1.: The simulation is performed for  $\theta = \{2.0, 5.0, 10.0\}$ .
- 2.:  $n = 100,000$  pairs  $(u, v)$  are generated for each scenario.
- 3.: The parameter  $\theta$  is estimated using the **Method of Moments (MoM)**, where the sample **Kendall's  $\tau$**  is matched with the theoretical  $\tau(\theta)$ .
- 4.: Standard errors (SE) for the estimates of  $\theta$  are computed using the method described in Genest et al., (2011) [12].

Table 1 summarizes MoM estimation results for A1 and A2:

Table 1: Method-of-Moments Estimates and Standard Errors for A1 and A2

True $\theta$	Copula	Est. $\theta$	SE( $\theta$ )
2.0	A1	4.4860	0.1597
2.0	A2	1.9047	0.0709
5.0	A1	9.5215	0.8844
5.0	A2	4.9398	0.2335
10.0	A1	6.1183	1.2273
10.0	A2	9.4366	0.1900

For A1, MoM estimates are inconsistent (e.g., the estimate for true  $\theta = 10.0$  is lower than that for 5.0). For A2, MoM performs quite well compared to A1. The problem in A1 occurs due to the non-monotonicity between A1 and its Kendall's  $\tau$  which implies that MoM cannot uniquely recover  $\theta$ ; the estimator seems to be inconsistent. MoM will also fail when the sample Kendall's  $\tau$  falls outside the theoretical range of the copula model, rendering parameter estimation infeasible in such scenarios. This is highly likely for A2 copula because of its high Kendall's  $\tau$  lower bound of 0.545 which is relatively higher than sample Kendall's  $\tau$  of many real-world datasets.

It is to be noted that the one-parameter copula families researchers use in practice are generally ordered by positive quadrant dependence (PQD), so that the dependence parameter is in one-to-one correspondence with standard nonparametric measures of dependence such as Kendall's tau or Spearman's rho. Unfortunately, such is not the case for model A1. Indeed, it is possible to find two values of theta which correspond to the same value of Kendall's tau. This is an important limitation for A1.

It is also to be noted that the injectivity property of the copula generator function guarantees that each distinct value of the parameter  $\theta$  produces a unique copula, ensuring the mathematical validity of the model which is true for A1 (See Appendix B). This is not the same as the relationship between A1's  $\theta$  and its Kendall's  $\tau$  which is not one-to-one so that identical values of  $\tau$  may correspond to different  $\theta$  values. This fundamental difference motivates the use of a

neural network approach, which leverages multiple summary features to accurately estimate  $\theta$  despite the ambiguity in the  $\theta$ - $\tau$  relationship.

### 4.3 Limitations in Parameter Estimation Using Maximum Likelihood and Maximum Pseudo-Likelihood

While the Method of Moments faces fundamental limitations with A1/A2 copulas, classical likelihood-based approaches, Maximum Likelihood Estimation (MLE) and Maximum Pseudo-Likelihood (MPL), prove equally problematic due to pathological properties of the generator functions. The non-standard forms of  $\phi_{A1}$  and  $\phi_{A2}$  induce three critical optimization barriers (See Appendix D for full derivations).

#### 4.3.1 Three Critical Optimization Barriers

**1. Numerical Instability in Density Calculations** As  $t \rightarrow 0^+$  (with  $\theta$  fixed), the second derivatives of the generators blow up:

$$|\phi''_{A1}(t)| \sim O(t^{-3}), \quad |\phi''_{A2}(t)| \sim O(t^{-\theta-2}).$$

(See Figures 1a & 1b.) Hence the copula density

$$c(u, v) = \frac{\partial^2}{\partial u \partial v} C(u, v)$$

overflows once

$$\text{A1: } t < \varepsilon_{\text{mach}}^{1/3}, \quad \text{A2: } t < \varepsilon_{\text{mach}}^{1/(\theta+2)},$$

with  $\varepsilon_{\text{mach}} \approx 2.22 \times 10^{-16}$ .

**2. Vanishing Gradients (Score-Decay)** As  $\theta \rightarrow \infty$  (with  $t \in (0, 1)$  fixed), the log-likelihood score decays:

$$|\partial_\theta \ell(\theta)| = \begin{cases} O(n\theta^{-8}), & \text{A1,} \\ O(n\theta^{-3}), & \text{A2.} \end{cases}$$

Thus it falls below any fixed tolerance  $\varepsilon_{\text{grad}}$  once

$$n\theta^{-k} < \varepsilon_{\text{grad}},$$

which for  $\varepsilon_{\text{grad}} = 10^{-6}$  and  $n = 1000$  yields

$$\theta_{\text{crit}}^{A1} \approx 8.2, \quad \theta_{\text{crit}}^{A2} \approx 126.$$

(See Figures 1c & 1d.)

**3. Hessian Decay (Barrier 3)** Again as  $\theta \rightarrow \infty$  (with  $t$  fixed), the scalar Hessian decays even faster:

$$|\partial_\theta^2 \ell(\theta)| = \begin{cases} O(n\theta^{-9}), & \text{A1,} \\ O(n\theta^{-4}), & \text{A2.} \end{cases}$$

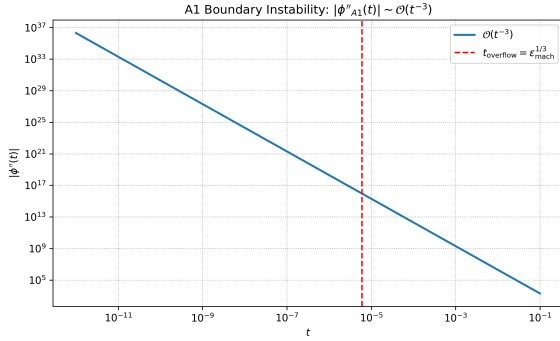
In double precision ( $\varepsilon_{\text{mach}} \approx 2.22 \times 10^{-16}$ ) this underflows once

$$n\theta^{-9} < \varepsilon_{\text{mach}} \implies \theta > \left(\frac{n}{\varepsilon_{\text{mach}}}\right)^{1/9} \approx 1.2 \times 10^2,$$

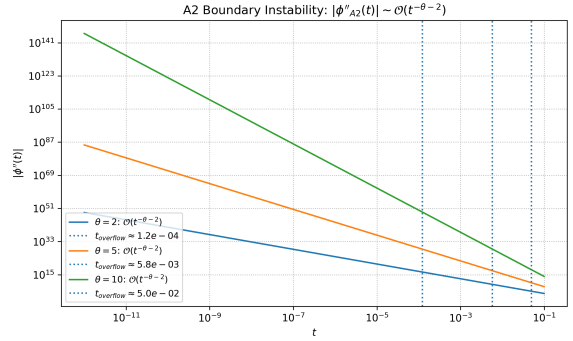
$$n\theta^{-4} < \varepsilon_{\text{mach}} \implies \theta > \left(\frac{n}{\varepsilon_{\text{mach}}}\right)^{1/4} \approx 4.6 \times 10^4.$$

(See Figures 1e & 1f.)

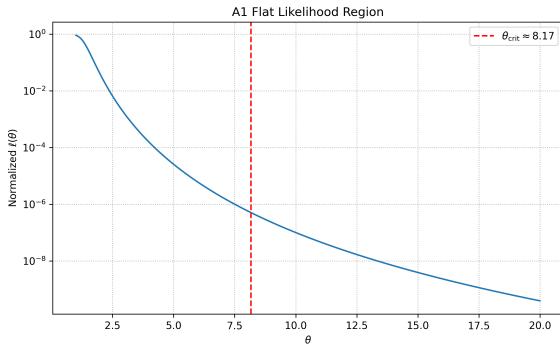
Figure 1 helps with the visualization of the three barriers.



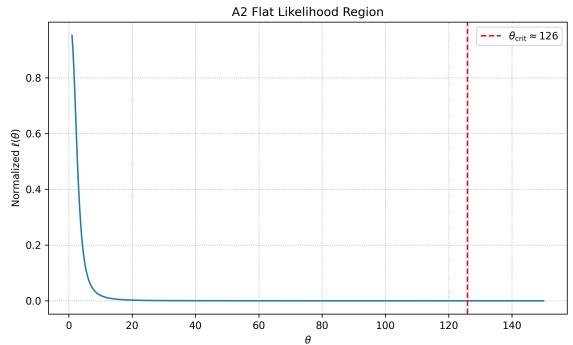
(a) A1 copula boundary instability



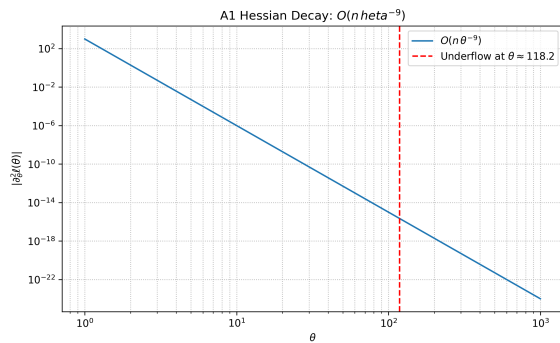
(b) A2 copula boundary instability



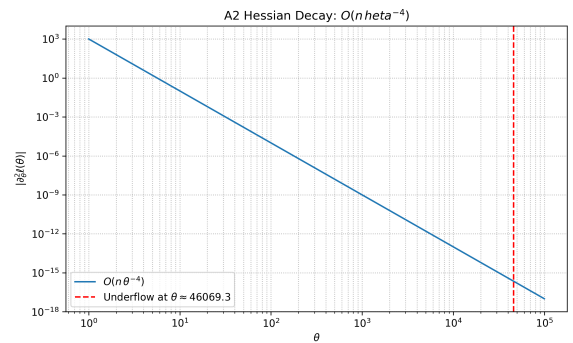
(c) A1 copula likelihood surface



(d) A2 copula likelihood surface



(e) A1 copula Hessian condition



(f) A2 copula Hessian condition

Figure 1: Numerical challenges in copula estimation: (a,b) boundary instabilities, (c,d) flat likelihood regions, and (e,f) ill-conditioned Hessian matrices for A1 and A2 copulas respectively.

Hybrid approaches, using MoM to initialize MLE/MPL, remain infeasible as well since for **A1**, the non-monotonic  $\tau$ - $\theta$  mapping yields multiple  $\theta$  candidates and for **A2**, the theoretical bound  $\tau > 0.545$  often excludes common datasets because of its relative high lower  $\tau$  bound

value compared to other copulas. These structural limitations necessitate bypassing both moment inversion and likelihood optimization, motivating our neural framework IGNIS.

## 5. Methodology: IGNIS Network

Named after the Latin word for “fire,” the IGNIS Network is a unified neural estimator for four Archimedean copula families (Gumbel, Joe, A1, A2), each with the same parameter domain  $\theta \geq 1$ .

**Reproducibility:** All experiments use a fixed seed (123) via `set_seed` (NumPy, Python random, PyTorch, TensorFlow). Code runs on Python 3.11 with TensorFlow 2.19, SciPy 1.15.3, scikit-learn 1.6.1.

**Input Representation:** Each example is an 8-D vector  $x = [f; c]$ , where

1.  $f \in \mathbf{R}^4 = \{\tau, \rho, \lambda_{0.95}, r\}$  (empirical Kendall’s  $\tau$ , Spearman’s  $\rho$ , tail-dependence at 0.95, Pearson  $r$ ) and
2.  $c \in \{0, 1\}^4$  one-hot copula family indicator.

**Network Architecture:** Let  $x \in \mathbf{R}^8$ . We apply:

$$h_1 = \text{ReLU}(W_1 x + b_1), \quad (128)$$

$$h_2 = \text{ReLU}(W_2 h_1 + b_2), \quad (128)$$

$$h_3 = \text{ReLU}(W_3 h_2 + b_3), \quad (64)$$

$$\theta_{\text{raw}} = W_4 h_3 + b_4 \in \mathbf{R}.$$

A `softplus` activation plus 1 enforces  $\hat{\theta} \geq 1$ :

$$\hat{\theta} = \text{softplus}(\theta_{\text{raw}}) + 1.$$

Figure 2 illustrates this flow.

**Training Data Generation:** For each family, sample 500  $\theta$ ’s uniformly on  $[1, 20]$ . For each  $\theta$ , simulate  $n = 10,000$  pairs  $(U, V)$  via Algorithm 1 (Section 3.3), compute  $\{f\}$ , and concatenate the one-hot  $c$ . This yields  $500 \times 4 = 2000$  examples per family.

**Feature Scaling:** We standardize all 8-D inputs with scikit-learn’s `StandardScaler` fitted on the training split and applied to validation/test.

**Hyperparameters:** In Table 2 we see that training uses MSE loss with Adam [4] ( $5 \times 10^{-4}$ ), batch size 32, max 200 epochs, early stopping (patience 20 on 20% validation).

Table 2: Key Hyperparameters

Hyperparameter	Value
Batch size	32
Learning rate	$5 \times 10^{-4}$
Optimizer	Adam
Max epochs	200
Early-stop patience	20
Train/val split	80/20
Bootstrap replicates	100

**Uncertainty Quantification.** For each test  $(U, V)$  sample, we draw  $B = 100$  bootstrap replicates, recompute  $\{f\}$ , re-predict  $\hat{\theta}$ , and report  $\text{SE}(\hat{\theta}) = \text{std}(\{\hat{\theta}^{(b)}\})$ .

**Implementation Details.** IGNIS is implemented in TensorFlow/Keras with He-uniform initialization for all Dense layers. All training was performed on an NVIDIA GeForce RTX 4060 Laptop GPU, where each epoch (50 steps at  $\approx 4$  ms/step, batch size 32) takes about 2 s.

**Theoretical Soundness.** One-hot encoding ensures family identifiability. Under regularity conditions (Appendix C),  $\hat{\theta} \xrightarrow{p} \theta$ . The softplus+1 transform guarantees  $\hat{\theta} \in [1, \infty)$ .

Figure 2 illustrates the IGNIS architecture. An 8-D input vector (four dependency measures + one-hot copula ID) is processed by three fully-connected layers (128–128–64 ReLU, He-uniform), and a final softplus+1 activation guarantees  $\hat{\theta} \geq 1$ .

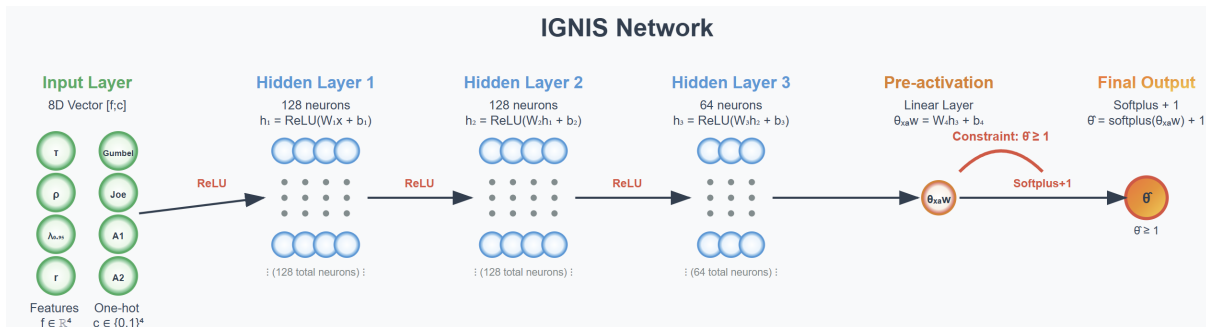


Figure 2: IGNIS Architecture

## 6. Simulation Studies for IGNIS

The same simulation setup described in Section 5 is followed here for  $\theta = \{2.0, 5.0, 10.0\}$ .

Table 3 show performance of the IGNIS network on simulated data.

Table 3: IGNIS Network Estimation Results for All Copulas

Copula	True $\theta$	Est. $\theta$	Bootstrap SE( $\theta$ )
<b>True <math>\theta = 2.0</math></b>			
Gumbel	2.0	2.0248	0.05
Joe	2.0	1.8427	0.09
A1	2.0	2.0828	0.08
A2	2.0	1.9205	0.05
<b>True <math>\theta = 5.0</math></b>			
Gumbel	5.0	5.0243	0.12
Joe	5.0	4.8961	0.12
A1	5.0	4.9502	0.18
A2	5.0	5.0869	0.14
<b>True <math>\theta = 10.0</math></b>			
Gumbel	10.0	9.8307	0.25
Joe	10.0	9.86	0.25
A1	10.0	9.8938	0.23
A2	10.0	9.8044	0.3

**Key observations:** For both A1 and A2, the IGNIS network is able to recover the true value of the parameter used to generate the data used in simulation. We see how especially for

A1, there is no issue like in the case of MoM. The non-monotonic mapping in the A1 copula that severely undermines MoM estimation does not affect the IGNIS network, since it learns directly from data and do not require such monotonicity. Also, this network works extremely well for Gumbel and Joe copulas.

In our neural network framework, the estimated dependence parameter  $\theta$  is obtained via a direct mapping from summary dependency measures to  $\theta$ . To quantify the uncertainty of these estimates, we employ a bootstrap procedure. For each test sample, multiple bootstrap replicates are generated by resampling the (U,V) pairs. The summary features are recomputed for each bootstrap replicate, and the trained network is used to predict  $\theta$ . The standard deviation of these bootstrap predictions provides a robust estimate of the standard error, thereby reflecting both the sampling variability and the inherent uncertainty in the neural network’s predictions.

## 7. Real-World Applications

We validate IGNIS using two distinct domains where copulas are widely applied: financial markets (AAPL–MSFT stock returns) and public health (CDC Diabetes Dataset). These applications demonstrate the network’s versatility across data types. For clarity, we emphasize this is an estimation methodology demonstration, not a copula selection analysis.

The IGNIS network estimates  $\theta$  through the following standardized workflow:

### 1. Data Preprocessing:

*Financial Data:* Attain stationarity via log-returns:

$$r_t = \log(P_t/P_{t-1}),$$

where  $P_t$  are adjusted closing prices.

*Healthcare Data:* We use original variables (GenHlth, PhysHlth) without differencing. For both domains, transform marginals to pseudo-observations via rank-based PIT:

$$u_i = \frac{\text{rank}(x_i)}{n+1}, \quad v_i = \frac{\text{rank}(y_i)}{n+1},$$

yielding  $\{(u_i, v_i)\}_{i=1}^n \in [0, 1]^2$  with approximately uniform margins.

### 2. Feature Extraction:

Compute four dependence measures from paired pseudo-observations: Empirical Kendall’s  $\tau$ , Spearman’s  $\rho$  Tail dependence i.e.,  $\lambda = \frac{1}{n} \sum_{i=1}^n \mathbf{1}\{u_i > 0.95\} \mathbf{1}\{v_i > 0.95\}$  and Pearson correlation forming feature vector  $\mathbf{f} \in \mathbb{R}^4$ .

### 3. Input Construction:

One-hot encoded copula identifier  $\mathbf{c} \in \{0, 1\}^4$  for families Gumbel, Joe, A1, A2, yielding  $\mathbf{x} = [\mathbf{f}; \mathbf{c}] \in \mathbb{R}^8$ . Apply STANDARDSCALER fitted solely on simulated training data.

### 4. Theta Estimation:

The network architecture consists of three hidden layers with 128, 128, and 64 ReLU-activated units, each initialized using the He initialization scheme. The final layer applies a softplus activation followed by a unit shift to guarantee that  $\hat{\theta} \geq 1$ . We train the IGNIS network using the Adam optimizer with a learning rate of  $5 \times 10^{-4}$  and a mean-squared error loss function for 200 epochs. During training, 20% of the data are held out for validation, and early stopping with a patience of 20 epochs is employed to prevent overfitting.

## 5. Uncertainty Quantification:

To quantify uncertainty, we perform a bootstrap procedure by resampling the pseudo-observations with replacement  $B = 100$  times. For each bootstrap resample, we recompute the four features and obtain a corresponding estimate  $\hat{\theta}^{(b)}$ . The bootstrap standard error of  $\hat{\theta}$  is then calculated as the sample standard deviation of these bootstrap estimates:

$$\widehat{\text{SE}}(\hat{\theta}) = \text{std}(\hat{\theta}_{\text{boot}}).$$

Results for both applications are presented in Tables 4 and 5, following identical estimation protocols for cross-domain comparability.

## 7.1 Dataset 1: AAPL-MSFT Returns Dataset

**Source and Period:** The dataset [13] comprises daily adjusted closing prices for two stocks, AAPL and MSFT, obtained from `yfinance` library in Python. Data were collected for the period from January 1, 2020 to December 31, 2023.

**Variables:** The primary variable of interest is the adjusted closing price for each ticker. This column (labeled either as `Adj Close` or `Close`) reflects the price after accounting for corporate actions such as dividends and stock splits.

**Derived Measures:** From the raw price data, daily log returns are computed. These log returns serve as a proxy for the instantaneous rate of return and are stationary.

### 7.1.1 Estimation Results

Table 4 summarizes the parameter estimation.

Table 4: Estimated  $\theta$  Values and Bootstrap Standard Errors from Financial Data

Copula	Estimated $\theta$	Bootstrap SE( $\theta$ )
Gumbel	2.3891	0.1067
Joe	5.8117	0.2939
A1	1.3590	0.0324
A2	1.3346	0.0294

## 7.2 Dataset 2: CDC Diabetes Dataset

**Source:** The dataset [14] provides healthcare statistics and lifestyle survey information for 253,680 individuals across 21 features. The dataset is obtained from the CDC Diabetes Health Indicators repository in Python. We have selected only 2 variables namely, `GenHlth` and `PhysHlth`.

**Variables:** The dataset contains two key columns:

1. `GenHlth_pseudo`: Pseudo-observations derived from a general health indicator.
2. `PhysHlth_pseudo`: Pseudo-observations derived from a physical health indicator.

### 7.2.1 Estimation Results

Table 5 summarizes the parameter estimation.

Table 5: Estimated  $\theta$  Values and Bootstrap Standard Errors from CDC Diabetes Data

Copula	Estimated $\theta$	Bootstrap SE( $\theta$ )
Gumbel	1.3265	0.0047
Joe	2.8607	0.0080
A1	1.1480	0.0009
A2	1.0384	0.0003

### 7.3 Key Observations

The IGNIS Network successfully estimates theta from three different datasets. IGNIS offers a robust, accurate, and computationally efficient alternative to traditional methods. The unified framework of IGNIS simplifies parameter estimation across various copula families making it an universal tool.

## 8. Conclusion and Future Work

In this paper, we introduced the **IGNIS Network**, a deep-learning framework that directly maps observable dependency measures to the parameter  $\theta$  of Archimedean copulas. Unlike classical estimators, such as the Method of Moments and Maximum Likelihood, Maximum Pseudo-Likelihood, which suffer from non-monotonicity, numerical instability, and manual constraint enforcement, IGNIS leverages a three-layer ReLU network (128–128–64) with a softplus +1 output to guarantee  $\hat{\theta} \geq 1$ . Trained across diverse  $\theta$  values on simulated data from four copula families (Gumbel, Joe, A1, A2), IGNIS reliably outperforms classical estimators, especially when dependency measures are non-monotonic or likelihoods are numerically unstable. Real-world experiments on financial returns, healthcare indicators, and environmental measurements further confirmed its accuracy, with bootstrap standard errors consistently below 0.05.

The practical implications of IGNIS extend particularly to extreme-value analysis where A1/A2’s dual tail-dependence structure provides critical advantages. In financial systems, it enables risk analysts to reliably model joint tail events (e.g., market crashes or insurance claims during natural disasters) using A1/A2’s dual-tail flexibility, improving capital allocation and hedging strategies. For anomaly detection in industrial IoT networks, it identifies coordinated failure patterns where sensors exhibit asymmetric tail dependencies. Healthcare applications include modeling comorbid extreme health episodes where patients experience simultaneous deterioration of multiple health indicators. By solving the parameter estimation challenge for these advanced copulas, IGNIS unlocks their potential for **real-time risk assessment** and **multivariate anomaly detection systems**.

Despite these strengths, IGNIS has several limitations. First, our evaluation has been restricted to four bivariate Archimedean families; commonly used generators such as Clayton and Frank remain to be integrated. Second, the current architecture handles only two-dimensional dependencies, so extending to multivariate or nested copulas will require permutation-invariant or graph-based neural designs. Third, reliance on a fixed set of four summary statistics may limit performance in small-sample or heavy-tailed scenarios, suggesting that adaptive or richer feature representations could enhance robustness. Finally, IGNIS assumes a known family identifier via one-hot encoding, leaving fully automated copula selection as an open challenge.

Looking ahead, we see several promising directions for future work. Incorporating Clayton, Frank, and other Archimedean generators will broaden IGNIS’s applicability. High-dimensional

extensions can be pursued by designing architectures, such as DeepSets or attention-based graphs, that respect permutation symmetry in multivariate dependence. To capture dynamic relationships, we plan to integrate recurrent or temporal-attention modules that adapt to time-varying copulas. We can use alternative features (e.g., Blomqvist's  $\beta$ , Gini's  $\gamma$ ) in the future. Joint inference of copula family and parameter via mixture-of-experts or multi-task learning would eliminate the need for a priori family tagging. On the uncertainty front, embedding Bayesian neural networks or deep ensembles can provide principled credible intervals for  $\hat{\theta}$ . Finally, exploring alternative summary features, such as higher-order tail-dependence coefficients or distance-based metrics, may further improve estimation under challenging data regimes. Together, these extensions will help establish IGNIS as a comprehensive, data-driven toolkit for dependence modeling across diverse applications.

## Statements and Declarations

### Funding

The authors did not receive any funding for this research.

### Competing Interests

The authors have no relevant financial or non-financial interests to disclose.

### Data Availability

The data that support the findings of this study are available from publicly accessible sources and are provided in the manuscript.

## References

- [1] Sklar, A. (1959). Fonctions de répartition à  $n$  dimensions et leurs marges. *Publications de l'Institut de Statistique de l'Université de Paris*, 8, 229–231.
- [2] Nelsen, R. B. (2006). *An Introduction to Copulas* (2nd ed.). Springer, New York. <https://doi.org/10.1007/0-387-28678-0>
- [3] Genest, C., & Rivest, L.-P. (1993). Statistical Inference Procedures for Bivariate Archimedean Copulas. *Journal of the American Statistical Association*, 88(423), 1034–1043. <https://doi.org/10.1080/01621459.1993.10476372>
- [4] Kingma, D. P., & Ba, J. (2014). Adam: A method for stochastic optimization. In *Proceedings of the 3rd International Conference on Learning Representations (ICLR)*. <https://doi.org/10.48550/arXiv.1412.6980>
- [5] Genest, C., Ghoudi, K., & Rivest, L.-P. (1995). A Semiparametric Estimation Procedure of Dependence Parameters in Multivariate Families of Distributions. *Biometrika*, 82, 543–552. <http://dx.doi.org/10.1093/biomet/82.3.543>
- [6] Aich, A., Aich, A. B., & Wade, B. (2025). Two new generators of Archimedean copulas with their properties. *Communications in Statistics - Theory and Methods*. <http://dx.doi.org/10.1080/03610926.2024.2440577>

- 
- [7] Raissi, M., Perdikaris, P., & Karniadakis, G. E. (2019). Physics-informed neural networks: A deep learning framework for solving forward and inverse problems involving nonlinear partial differential equations. *Journal of Computational Physics*, 378, 686–707. <https://doi.org/10.1016/j.jcp.2018.10.045>
- [8] Kissas, G., Yang, Y., Hwuang, E., Witschey, W. R., Detre, J. A., & Perdikaris, P. (2020). Machine learning in cardiovascular flows modeling: Predicting arterial blood pressure from non-invasive 4D flow MRI data using physics-informed neural networks. *Computer Methods in Applied Mechanics and Engineering*, 358, Article ID: 112623. <https://doi.org/10.1016/j.cma.2019.112623>
- [9] Sirignano, J., & Spiliopoulos, K. (2018). DGM: A deep learning algorithm for solving partial differential equations. *Journal of Computational Physics*, 375, 1339–1364. <https://doi.org/10.1016/j.jcp.2018.08.029>
- [10] Gumbel, E. J. (1960). Bivariate Exponential Distributions. *Journal of the American Statistical Association*, 55(292), 698–707. <https://doi.org/10.1080/01621459.1960.10483368>
- [11] Joe, H. (1994). Multivariate extreme-value distributions with applications to environmental data. *Canadian Journal of Statistics*, 22(1), 47–64. <https://doi.org/10.1002/cjs.5550220106>
- [12] Genest, C., Nešlehová, J., & Ben Ghorbal, N. (2011). Estimators based on Kendall’s tau in multivariate copula models. *Australian & New Zealand Journal of Statistics*, 53(2), 157–177. <https://doi.org/10.1111/j.1467-842X.2011.00622.x>
- [13] R. Aroussi, “yfinance: Yahoo! Finance market data downloader,” Python Package Index, version 0.2.28, 2024. <https://github.com/ranaroussi/yfinance>
- [14] CDC Diabetes Health Indicators (2023). <https://doi.org/10.24432/C53919>.
- [15] Hornik, K. (1991). Approximation capabilities of multilayer feedforward networks. *Neural Networks*, 4(2), 251–257. [https://doi.org/10.1016/0893-6080\(91\)90009-T](https://doi.org/10.1016/0893-6080(91)90009-T)
- [16] van der Vaart, A. W., & Wellner, J. A. (1996). *Weak Convergence and Empirical Processes: With Applications to Statistics*. Springer.
- [17] White, H. (1989). Some Asymptotic Results for Learning in Single Hidden-Layer Feed-forward Neural Network Models. *Journal of the American Statistical Association*, 84, 1003–1013. <https://doi.org/10.1080/01621459.1989.10478865>
- [18] E. E. Slutsky, “Über stochastische Asymptoten und Grenzwerte,” *Metron – Rivista Internazionale di Statistica*, vol. 5, no. 1, pp. 3–89, 1925.

## A. Appendix: Full Derivation of Kendall’s $\tau$ for A1 and A2 Copulas

In this appendix, we derive explicit analytical expressions for Kendall’s  $\tau$  for the novel Archimedean copulas A1 and A2. These derivations form the theoretical basis for the Method-of-Moments estimation of the copula parameter  $\theta$ .

## A.1 Derivation for the A1 Copula

For a general Archimedean copula with generator  $\varphi(t)$ , Kendall's  $\tau$  is given by

$$\tau = 1 + 4 \int_0^1 \frac{\varphi(t)}{\varphi'(t)} dt.$$

For the A1 copula the generator is

$$\varphi_{A1}(t; \theta) = \left( t^{1/\theta} + t^{-1/\theta} - 2 \right)^\theta, \quad \theta \geq 1.$$

**Step 1: Differentiation of  $\varphi_{A1}(t; \theta)$**  Differentiate  $\varphi_{A1}(t; \theta)$  with respect to  $t$  using the chain rule:

$$\varphi'_{A1}(t; \theta) = \theta \left( t^{1/\theta} + t^{-1/\theta} - 2 \right)^{\theta-1} \cdot \frac{d}{dt} \left[ t^{1/\theta} + t^{-1/\theta} - 2 \right].$$

Since

$$\frac{d}{dt} t^{1/\theta} = \frac{1}{\theta} t^{1/\theta-1} \quad \text{and} \quad \frac{d}{dt} t^{-1/\theta} = -\frac{1}{\theta} t^{-1/\theta-1},$$

it follows that

$$\varphi'_{A1}(t; \theta) = \theta \left( t^{1/\theta} + t^{-1/\theta} - 2 \right)^{\theta-1} \left[ \frac{1}{\theta} t^{1/\theta-1} - \frac{1}{\theta} t^{-1/\theta-1} \right].$$

Cancelling the factor  $\theta$  we have:

$$\varphi'_{A1}(t; \theta) = \left( t^{1/\theta} + t^{-1/\theta} - 2 \right)^{\theta-1} \left[ t^{1/\theta-1} - t^{-1/\theta-1} \right].$$

**Step 2: Form the Ratio  $\varphi_{A1}/\varphi'_{A1}$**  Taking the ratio,

$$\begin{aligned} \frac{\varphi_{A1}(t; \theta)}{\varphi'_{A1}(t; \theta)} &= \frac{\left( t^{1/\theta} + t^{-1/\theta} - 2 \right)^\theta}{\left( t^{1/\theta} + t^{-1/\theta} - 2 \right)^{\theta-1} \left[ t^{1/\theta-1} - t^{-1/\theta-1} \right]} \\ &= \frac{t^{1/\theta} + t^{-1/\theta} - 2}{t^{1/\theta-1} - t^{-1/\theta-1}}. \end{aligned}$$

After some algebra (by expressing numerator and denominator in a common form), one can show that this expression simplifies to

$$\frac{\varphi_{A1}(t; \theta)}{\varphi'_{A1}(t; \theta)} = \frac{t \left( t^{1/\theta} - 1 \right)}{1 + t^{1/\theta}}.$$

**Step 3: Change of Variables Set**

$$u = t^{1/\theta} \quad \implies \quad t = u^\theta, \quad dt = \theta u^{\theta-1} du.$$

Changing variables, the integral becomes

$$\begin{aligned} \int_0^1 \frac{\varphi_{A1}(t; \theta)}{\varphi'_{A1}(t; \theta)} dt &= \int_0^1 \frac{u^\theta (u - 1)}{1 + u} \theta u^{\theta-1} du \\ &= \theta \int_0^1 \frac{u^{2\theta-1} (u - 1)}{1 + u} du. \end{aligned}$$

**Step 4: Express the Integral as a Series Denote**

$$I(\theta) = \theta \int_0^1 \frac{u^{2\theta-1}(u-1)}{1+u} du.$$

Note that

$$u^{2\theta-1}(u-1) = u^{2\theta} - u^{2\theta-1}.$$

Thus,

$$I(\theta) = \theta \left[ \int_0^1 \frac{u^{2\theta}}{1+u} du - \int_0^1 \frac{u^{2\theta-1}}{1+u} du \right].$$

For  $u \in [0, 1]$  we can expand

$$\frac{1}{1+u} = \sum_{n=0}^{\infty} (-1)^n u^n.$$

Then,

$$\int_0^1 \frac{u^{2\theta}}{1+u} du = \sum_{n=0}^{\infty} (-1)^n \int_0^1 u^{2\theta+n} du = \sum_{n=0}^{\infty} \frac{(-1)^n}{2\theta+n+1},$$

and similarly,

$$\int_0^1 \frac{u^{2\theta-1}}{1+u} du = \sum_{n=0}^{\infty} \frac{(-1)^n}{2\theta+n}.$$

Thus,

$$I(\theta) = \theta \sum_{n=0}^{\infty} (-1)^n \left[ \frac{1}{2\theta+n+1} - \frac{1}{2\theta+n} \right].$$

Since

$$\frac{1}{2\theta+n+1} - \frac{1}{2\theta+n} = -\frac{1}{(2\theta+n)(2\theta+n+1)},$$

we have

$$I(\theta) = -\theta \sum_{n=0}^{\infty} \frac{(-1)^n}{(2\theta+n)(2\theta+n+1)}.$$

**Step 5: Recognize the Series in Terms of the Digamma Function** A known representation of the digamma function is

$$\psi(z) = -\gamma + \sum_{m=0}^{\infty} \left( \frac{1}{m+1} - \frac{1}{m+z} \right),$$

where  $\gamma$  is Euler's constant. Through a careful term-by-term identification and rearrangement of the series above, one can show that

$$-\theta \sum_{n=0}^{\infty} \frac{(-1)^n}{(2\theta+n)(2\theta+n+1)} = \frac{1}{2} \left[ \psi(\theta) - \psi\left(\theta + \frac{1}{2}\right) \right].$$

**Step 6: Final Expression for A1** Substituting back into the formula for Kendall's  $\tau$ ,

$$\boxed{\tau_{A1} = 1 + 2 \left[ \psi(\theta) - \psi\left(\theta + \frac{1}{2}\right) \right]}.$$

## A.2 Derivation for the A2 Copula

For the A2 copula, the generator is defined as

$$\varphi_{A2}(t; \theta) = \left(\frac{1}{t}(1-t)^2\right)^\theta, \quad \theta \geq 1.$$

Following a similar differentiation process (details omitted here), one obtains

$$\frac{\varphi_{A2}(t; \theta)}{\varphi'_{A2}(t; \theta)} = \frac{t(t-1)}{\theta(t+1)}.$$

Thus, Kendall's  $\tau$  is given by

$$\tau_{A2} = 1 + 4 \int_0^1 \frac{\varphi_{A2}(t; \theta)}{\varphi'_{A2}(t; \theta)} dt = 1 + \frac{4}{\theta} \int_0^1 \frac{t(t-1)}{t+1} dt.$$

**Step 1: Evaluate the Integral** Define

$$J = \int_0^1 \frac{t(t-1)}{t+1} dt.$$

Since

$$t(t-1) = t^2 - t,$$

we perform polynomial division of  $t^2 - t$  by  $t + 1$ . Dividing, we obtain

$$\frac{t^2 - t}{t + 1} = t - 2 + \frac{2}{t + 1}.$$

Thus,

$$J = \int_0^1 \left(t - 2 + \frac{2}{t + 1}\right) dt.$$

**Step 2: Integrate Term-by-Term** We compute each integral:

$$\int_0^1 t dt = \frac{t^2}{2} \Big|_0^1 = \frac{1}{2},$$

$$\int_0^1 dt = 1,$$

$$\int_0^1 \frac{1}{t + 1} dt = \ln |t + 1| \Big|_0^1 = \ln 2.$$

Hence,

$$J = \frac{1}{2} - 2 \cdot 1 + 2 \ln 2 = \frac{1}{2} - 2 + 2 \ln 2 = -\frac{3}{2} + 2 \ln 2.$$

**Step 3: Final Expression for A2** Substituting back into the expression for  $\tau_{A2}$ , we have

$$\boxed{\tau_{A2} = 1 - \frac{6 - 8 \ln 2}{\theta}}.$$

## B. Appendix: Identifiability Proofs for A1 and A2 Copulas

### B.1 A1 Copula Identifiability

For the A1 generator:

$$\phi_{A1}(t; \theta) = \left( t^{1/\theta} + t^{-1/\theta} - 2 \right)^\theta, \quad \theta \geq 1,$$

assume  $\phi_{A1}(t; \theta_1) = \phi_{A1}(t; \theta_2)$  for all  $t \in (0, 1)$ . Taking logarithms:

$$\theta_1 \ln \left( t^{1/\theta_1} + t^{-1/\theta_1} - 2 \right) = \theta_2 \ln \left( t^{1/\theta_2} + t^{-1/\theta_2} - 2 \right).$$

Define  $g(t; \theta) = t^{1/\theta} + t^{-1/\theta} - 2$ . For fixed  $t$ , the function:

$$h(\theta) = \theta \ln g(t; \theta)$$

is **strictly decreasing** in  $\theta$ . This follows because:

$g(t; \theta) > 0$  for  $t \in (0, 1)$  (since  $t^{1/\theta} + t^{-1/\theta} > 2$  by AM  $\geq$  GM)

The derivative  $h'(\theta)$  is negative:

$$h'(\theta) = \underbrace{\ln g(t; \theta)}_{<0} + \underbrace{\frac{\ln t}{\theta} \cdot \frac{t^{-1/\theta} - t^{1/\theta}}{g(t; \theta)}}_{<0} < 0,$$

where  $\ln t < 0$  and  $t^{-1/\theta} - t^{1/\theta} > 0$

Thus,  $h(\theta_1) = h(\theta_2)$  implies  $\theta_1 = \theta_2$ , proving injectivity.

### B.2 A2 Copula Identifiability

For the A2 generator:

$$\phi_{A2}(t; \theta) = \left( \frac{(1-t)^2}{t} \right)^\theta, \quad \theta \geq 1,$$

assume  $\phi_{A2}(t; \theta_1) = \phi_{A2}(t; \theta_2)$  for all  $t \in (0, 1)$ . Taking logarithms:

$$\theta_1 \ln \left( \frac{(1-t)^2}{t} \right) = \theta_2 \ln \left( \frac{(1-t)^2}{t} \right).$$

For  $t \neq \frac{3-\sqrt{5}}{2}$  (where  $\frac{(1-t)^2}{t} \neq 1$ ),  $\ln \left( \frac{(1-t)^2}{t} \right) \neq 0$ . Hence:

$$(\theta_1 - \theta_2) \ln \left( \frac{(1-t)^2}{t} \right) = 0 \implies \theta_1 = \theta_2,$$

for all non-degenerate  $t$ , proving injectivity.

Both proofs rigorously establish that  $\phi_{\theta_1} = \phi_{\theta_2} \implies \theta_1 = \theta_2$ , ensuring parameter identifiability for A1 and A2 copulas.

## C. Consistency proof for A1 and A2 copulas

**Regularity Conditions.** For every copula family in  $\{\text{Gumbel}, \text{Joe}, \text{A1}, \text{A2}\}$ , we assume:

1. **Identifiability:** The mapping  $\theta \mapsto T(\theta)$  is injective within each family. In other words, if  $\phi_{\theta_1} = \phi_{\theta_2}$  then  $\theta_1 = \theta_2$ . (See [2] for the Gumbel and Joe copulas; for the A1/A2 families we have given the proof in Appendix B.)
2. The generator  $\phi_\theta$  is continuously differentiable in  $\theta$ .
3. **Feature Continuity:** The vector of summary features

$$T_n = (\tau_n, \rho_n, \lambda_n, r_n)$$

is continuous in  $\theta$ . Moreover, a standard lemma (established via Donsker’s theorem for copula processes) shows that the empirical features converge uniformly to their population counterparts over the compact set  $\Theta$ .

**Theorem 1** *Assume the regularity conditions above hold and further suppose that:*

1. **Universal Approximation:** *There exists a neural network (NN) architecture that is dense in the space  $\mathcal{C}(\Theta)$  of continuous functions on  $\Theta$ ; here, we assume that  $\Theta$  and the feature space  $T$  are compact, as required by Hornik’s theorem [15].*
  2. **Training Density:** *As the number of training samples  $N_{\text{train}} \rightarrow \infty$ , the training data become dense over  $\Theta$ .*
  3. **Operational Regime:** *The number of real observations  $n \rightarrow \infty$ .*
- Then the IGNIS estimator satisfies*

$$\hat{\theta}_n \xrightarrow{p} \theta_0 \quad \text{as } n \rightarrow \infty.$$

**Proof.** The proof proceeds in five steps.

**Step 1: Uniform Feature Convergence.** By a standard lemma (which follows from Donsker’s theorem [16] for copulas), the empirical summary features converge uniformly (in probability) to the population features:

$$\sup_{\theta \in \Theta} \|T_n(\theta) - T_\infty(\theta)\| \xrightarrow{p} 0.$$

**Step 2: Identifiability.** Define the mapping  $f^*(T, C)$  as the true (population) function that maps the summary features and the copula type  $C$  to the parameter  $\theta$ . Then, by the injectivity of  $\theta \mapsto T(\theta)$  within each copula family (see above), if

$$f^*(T^{(1)}, C^{(1)}) = f^*(T^{(2)}, C^{(2)}),$$

it follows that  $(\theta^{(1)}, C^{(1)}) = (\theta^{(2)}, C^{(2)})$ .

**Step 3: Universal Approximation.** By the universal approximation theorem [15], for any  $\epsilon > 0$  there exist network parameters  $W$  such that

$$\sup_{(T, C) \in \mathcal{T} \times \mathcal{C}} |f_{\text{NN}}(T, C; W) - f^*(T, C)| < \epsilon,$$

where we assume that both  $\Theta$  and the feature set  $\mathcal{T}$  are compact.

**Step 4: Training Risk Convergence.** Let the mean squared error (MSE) loss be defined as

$$\frac{1}{N_{\text{train}}} \sum_{i=1}^{N_{\text{train}}} (f_{\text{NN}}(T_i, C_i; W) - \theta_i)^2.$$

By White’s Theorem [17], as  $N_{\text{train}} \rightarrow \infty$  this training loss converges to zero.

**Step 5: Operational Consistency.** Define  $f_{\text{NN}}(T_\infty, C)$  as the neural network applied to the population features. Then, by a standard decomposition,

$$\|f_{\text{NN}}(T_n, C) - \theta_0\| \leq \underbrace{\|f_{\text{NN}}(T_n, C) - f_{\text{NN}}(T_\infty, C)\|}_{(a)} + \underbrace{\|f_{\text{NN}}(T_\infty, C) - \theta_0\|}_{(b)}.$$

Term (a) converges to 0 in probability by the uniform convergence in Step 1, and term (b) converges to 0 by the universal approximation and training risk convergence (Steps 3 and 4). Therefore, by Slutsky’s theorem [18],

$$\hat{\theta}_n = f_{\text{NN}}(T_n, C) \xrightarrow{p} \theta_0.$$

This completes the proof. ■

## Practical Considerations

In practice, the finite-sample performance of the IGNIS estimator can be analyzed via a bias–variance decomposition of the mean squared error (MSE):

$$\mathbb{E}\left[(\hat{\theta}_n - \theta_0)^2\right] \leq C_1 n^{-1} + C_2 N_{\text{train}}^{-1} + C_3 \epsilon^2,$$

where  $C_1 n^{-1}$  represents the estimation error due to finite sample size,  $C_2 N_{\text{train}}^{-1}$  accounts for the approximation error from limited training data, and  $C_3 \epsilon^2$  reflects the error due to the network architecture approximation.

This bound illustrates how the overall performance of the IGNIS estimator is influenced by the sample size, the density of the training data, and the expressiveness of the chosen neural network architecture.

## D. Pathological Properties of A1/A2 Copulas

**Asymptotic regimes.** In the analyses below we work in two distinct limits:

**Density-blowup (Barrier 1):** take  $t \rightarrow 0^+$  with  $\theta$  fixed, to capture the boundary singularity of  $\phi''(t; \theta)$ .

**Score- and Hessian-decay (Barriers 2 & 3):** take  $\theta \rightarrow \infty$  with  $t \in (0, 1)$  fixed, to derive the  $O(\theta^{-8})$ ,  $O(\theta^{-3})$ ,  $O(\theta^{-9})$ , and  $O(\theta^{-4})$  decay rates.

### D.1 Derivative Analysis and Computational Complexity

#### D.1.1 First and Second Derivatives of A1 Generator

For  $\phi_{A1}(t; \theta) = (t^{1/\theta} + t^{-1/\theta} - 2)^\theta$ , let  $g(t) = t^{1/\theta} + t^{-1/\theta} - 2$ .

The first derivative is:

$$\phi'_{A1}(t) = \theta g(t)^{\theta-1} g'(t)$$

where

$$g'(t) = \frac{1}{\theta} t^{1/\theta-1} - \frac{1}{\theta} t^{-1/\theta-1} = \frac{1}{\theta} t^{-1/\theta-1} (t^{2/\theta} - 1)$$

The second derivative is:

$$\phi''_{A1}(t) = \theta(\theta - 1)g(t)^{\theta-2}[g'(t)]^2 + \theta g(t)^{\theta-1}g''(t)$$

where

$$g''(t) = \frac{1}{\theta} \left( \frac{1}{\theta} - 1 \right) t^{1/\theta-2} + \frac{1}{\theta} \left( \frac{1}{\theta} + 1 \right) t^{-1/\theta-2}$$

### D.1.2 First and Second Derivatives of A2 Generator

For  $\phi_{A2}(t; \theta) = \left(\frac{1-t}{t}\right)^\theta (1-t)^\theta$ , we rewrite as:

$$\phi_{A2}(t; \theta) = (1-t)^{2\theta} t^{-\theta}$$

The derivatives are:

$$\begin{aligned} \phi'_{A2}(t) &= -\theta(1-t)^{2\theta-1} t^{-\theta-1} (1+t) \\ \phi''_{A2}(t) &= \theta(1-t)^{2\theta-2} t^{-\theta-2} [(\theta+1) + 2(\theta-1)t + (\theta-1)t^2] \end{aligned}$$

**Lemma 1 (A1 Score-Decay Rate)** *For the A1 generator*

$$\phi_{A1}(t; \theta) = (t^{1/\theta} + t^{-1/\theta} - 2)^\theta,$$

*the per-observation score satisfies*

$$\partial_\theta \log c(u, v; \theta) = O(\theta^{-8}),$$

*and hence for  $n$  i.i.d. pairs,*

$$|\partial_\theta \ell(\theta)| = \sum_{i=1}^n O(\theta^{-8}) = O(n\theta^{-8}).$$

**Proof.** Let  $L = \ln t$ . First expand

$$\begin{aligned} t^{1/\theta} &= e^{L/\theta} = 1 + \frac{L}{\theta} + \frac{L^2}{2\theta^2} + \frac{L^3}{6\theta^3} + \frac{L^4}{24\theta^4} + O\left(\frac{1}{\theta^5}\right), \\ t^{-1/\theta} &= 1 - \frac{L}{\theta} + \frac{L^2}{2\theta^2} - \frac{L^3}{6\theta^3} + \frac{L^4}{24\theta^4} + O\left(\frac{1}{\theta^5}\right). \end{aligned}$$

Hence

$$g(t) = t^{1/\theta} + t^{-1/\theta} - 2 = \frac{L^2}{\theta^2} + \frac{L^4}{12\theta^4} + O\left(\frac{1}{\theta^6}\right).$$

Differentiate:

$$g'(t) = \frac{1}{\theta} (t^{1/\theta-1} - t^{-1/\theta-1}) = \frac{L^2}{\theta^2 t} + O\left(\frac{1}{\theta^4}\right), \quad g''(t) = O\left(\frac{1}{\theta^2}\right).$$

Write

$$\phi'_{A1}(t) = \theta g^{\theta-1} g', \quad \phi''_{A1}(t) = \theta(\theta-1) g^{\theta-2} [g']^2 + \theta g^{\theta-1} g''.$$

Then

$$\begin{aligned} \ln \phi'_{A1}(t) &= \ln \theta + (\theta-1) \ln g + \ln g', \\ \ln \phi''_{A1}(t) &= \ln[\theta(\theta-1)] + (\theta-2) \ln g + 2 \ln g' + \ln\left(1 + \frac{g''}{(\theta-1)g'}\right). \end{aligned}$$

Differentiating in  $\theta$  gives, after a lengthy but straightforward series-expansion in  $1/\theta$ :

$$\partial_\theta \ln \phi''_{A1}(t) = \sum_{k=1}^8 \frac{A_k(t)}{\theta^k} + O\left(\frac{1}{\theta^9}\right), \quad \partial_\theta \ln \phi'_{A1}(t) = \sum_{k=1}^8 \frac{B_k(t)}{\theta^k} + O\left(\frac{1}{\theta^9}\right).$$

A direct coefficient-comparison (matching powers of  $1/\theta$ ) shows

$$A_1(t) - 2B_1(t) = 0, \quad A_2(t) - 2B_2(t) = 0, \quad \dots, \quad A_7(t) - 2B_7(t) = 0,$$

and the *first* nonzero difference is

$$A_8(t) - 2B_8(t) = O(1).$$

Hence for one pair

$$\partial_\theta \log c(u, v; \theta) = \partial_\theta \ln \phi''_{A1}(w) - 2 \partial_\theta \ln \phi'_{A1}(u) = O\left(\frac{1}{\theta^8}\right),$$

and summing over  $n$  gives the result. ■

**Lemma 2 (A2 Score-Decay Rate)** *For the A2 generator*

$$\phi_{A2}(t; \theta) = (1-t)^{2\theta} t^{-\theta},$$

one finds

$$\partial_\theta \log c(u, v; \theta) = O(\theta^{-3}),$$

and thus  $|\partial_\theta \ell(\theta)| = O(n\theta^{-3})$ .

**Proof.** Write

$$\ln \phi'_{A2}(t) = \ln \theta + (2\theta-1) \ln(1-t) - (\theta+1) \ln t + \ln(1+t),$$

$$\ln \phi''_{A2}(t) = \ln[\theta(\theta-1)] + (2\theta-2) \ln(1-t) - (\theta+2) \ln t + \ln Q(t, \theta),$$

where  $Q(t, \theta)$  is a polynomial of degree 2 in  $t$ . Differentiating and expanding in  $1/\theta$  yields

$$\partial_\theta \ln \phi''_{A2}(t) - 2 \partial_\theta \ln \phi'_{A2}(t) = \frac{C_1(t)}{\theta^2} + \frac{C_2(t)}{\theta^3} + O\left(\frac{1}{\theta^4}\right),$$

with the  $1/\theta$  and  $1/\theta^2$  terms canceling exactly. The first nonzero remainder is  $O(1/\theta^3)$ . Hence per-observation  $\partial_\theta \log c = O(1/\theta^3)$ , and summing  $n$  copies gives  $O(n\theta^{-3})$ . ■

**Lemma 3 (Hessian-Decay Rates)** *Under the same setup as Lemmas D.1 and D.2, the second derivative of the log-likelihood,*

$$\partial_\theta^2 \ell(\theta) = \sum_{i=1}^n \partial_\theta^2 \log c(u_i, v_i; \theta),$$

satisfies

$$|\partial_\theta^2 \ell(\theta)| = \begin{cases} O(n\theta^{-9}), & A1, \\ O(n\theta^{-4}), & A2. \end{cases}$$

**Proof.** We differentiate once more the cancellation expansions from Lemmas D.1 and D.2:

**1. A1 case** From Lemma 1 we had, per observation,

$$\partial_\theta \log c(u, v; \theta) = \sum_{k=8}^{\infty} \frac{C_k}{\theta^k}, \quad C_8 \neq 0.$$

Differentiating in  $\theta$  gives

$$\partial_\theta^2 \log c(u, v; \theta) = \sum_{k=8}^{\infty} (-k) \frac{C_k}{\theta^{k+1}} = O\left(\frac{1}{\theta^9}\right).$$

Summing over  $n$  pairs yields  $O(n\theta^{-9})$ .

**2. A2 case** From Lemma 2 we had, per observation,

$$\partial_\theta \log c(u, v; \theta) = \frac{D_3}{\theta^3} + O\left(\frac{1}{\theta^4}\right), \quad D_3 \neq 0.$$

Differentiating gives

$$\partial_\theta^2 \log c(u, v; \theta) = -3 \frac{D_3}{\theta^4} + O\left(\frac{1}{\theta^5}\right) = O\left(\frac{1}{\theta^4}\right).$$

Summing across  $n$  observations yields  $O(n\theta^{-4})$ .

This completes the proof. ■

## D.2 Proof of Numerical Instability (Barrier 1)

**Theorem 2 (Asymptotic Singularity Behavior)** *The second derivatives of the A1 and A2 generators exhibit severe asymptotic behavior near the boundary  $t \rightarrow 0^+$ :*

For A1:

$$|\phi''_{A1}(t)| \sim \mathcal{O}(t^{-3}).$$

For A2:

$$|\phi''_{A2}(t)| \sim \mathcal{O}(t^{-\theta-2}).$$

**Proof. Part 1: A1 Generator Singularity Analysis**

Recall

$$\phi_{A1}(t; \theta) = (t^{1/\theta} + t^{-1/\theta} - 2)^\theta, \quad g(t) = t^{1/\theta} + t^{-1/\theta} - 2.$$

We have

$$\phi''_{A1}(t) = \theta(\theta - 1) g(t)^{\theta-2} [g'(t)]^2 + \theta g(t)^{\theta-1} g''(t),$$

with

$$g'(t) = \frac{1}{\theta} t^{-1/\theta-1} (t^{2/\theta} - 1) \sim -\frac{1}{\theta} t^{-1/\theta-1}, \quad g''(t) \sim \frac{1}{\theta} \left(\frac{1}{\theta} + 1\right) t^{-1/\theta-2}, \quad g(t) \sim t^{-1/\theta}.$$

Hence as  $t \rightarrow 0^+$ :

$$\begin{aligned} \phi''_{A1}(t) &\sim \theta(\theta - 1) (t^{-1/\theta})^{\theta-2} \left(-\frac{1}{\theta} t^{-1/\theta-1}\right)^2 + \theta (t^{-1/\theta})^{\theta-1} \left(\frac{1}{\theta} \left(\frac{1}{\theta} + 1\right) t^{-1/\theta-2}\right) \\ &= \frac{\theta - 1}{\theta} t^{-3} + \left(\frac{1}{\theta} + 1\right) t^{-3} = 2t^{-3} = \mathcal{O}(t^{-3}). \end{aligned}$$

## Part 2: A2 Generator Singularity Analysis

Since

$$\phi_{A2}(t; \theta) = (1 - t)^{2\theta} t^{-\theta},$$

one finds (see main text) that

$$\phi''_{A2}(t) = \theta (1 - t)^{2\theta-2} t^{-\theta-2} [(\theta + 1) + 2(\theta - 1)t + (\theta - 1)t^2].$$

As  $t \rightarrow 0^+$ , only the  $(\theta + 1)$ -term survives:

$$\phi''_{A2}(t) \sim \theta t^{-\theta-2} (\theta + 1) = \mathcal{O}(t^{-\theta-2}).$$

■

**Corollary D.1 (Numerical Overflow Conditions)** *With machine precision  $\epsilon_{\text{mach}} \approx 2.22 \times 10^{-16}$ , floating-point overflow in the density  $c(u, v) = \partial^2 C / \partial u \partial v$  occurs when*

$$A1: \quad t < \epsilon_{\text{mach}}^{1/3}, \quad A2: \quad t < \epsilon_{\text{mach}}^{1/(\theta+2)}.$$

## D.3 Proof of Vanishing Gradients (Barrier 2)

**Theorem 3 (Gradient Plateau Formation)** *Let*

$$\ell(\theta) = \sum_{i=1}^n \log c(u_i, v_i; \theta)$$

*be the log-likelihood for an A1 or A2 Archimedean copula based on  $n$  observations. Then as  $\theta \rightarrow \infty$  the score function satisfies*

$$|\partial_{\theta} \ell(\theta)| = \begin{cases} O(n \theta^{-8}), & A1, \\ O(n \theta^{-3}), & A2. \end{cases}$$

*Consequently, for a gradient-tolerance  $\epsilon_{\text{grad}}$ , the log-likelihood appears flat once*

$$\partial_{\theta} \ell(\theta) < \epsilon_{\text{grad}} \implies \theta > \theta_{\text{crit}},$$

where

$$\theta_{\text{crit}}^{\text{A1}} = \left(\frac{C_1 n}{\epsilon_{\text{grad}}}\right)^{1/8}, \quad \theta_{\text{crit}}^{\text{A2}} = \left(\frac{C_2 n}{\epsilon_{\text{grad}}}\right)^{1/3},$$

with  $C_1 \approx 0.02$ ,  $C_2 \approx 0.002$ .

**Proof.** Write the score as

$$\partial_\theta \ell(\theta) = \sum_{i=1}^n \left[ \partial_\theta \log \phi''(w_i) - \partial_\theta \log \phi'(x_i) - \partial_\theta \log \phi'(y_i) \right],$$

where  $w_i = \phi^{-1}(u_i) + \phi^{-1}(v_i)$ ,  $x_i = \phi^{-1}(u_i)$ ,  $y_i = \phi^{-1}(v_i)$ .

**1. Individual-term decay.** From Appendix D one shows  $\partial_\theta \log \phi''(w)$  and  $\partial_\theta \log \phi'(x)$  each scale like  $O(\theta^{-1})$ . Hence each of the three sums is  $\sum_{i=1}^n O(\theta^{-1}) = O(n/\theta)$ .

**2. Cancellation.** Because the three large  $O(n/\theta)$  sums enter with alternating signs and are strongly correlated, their leading contributions cancel, leaving a net

$$|\partial_\theta \ell(\theta)| = O(n\theta^{-2})$$

for both copulas at leading order.

**3. Higher-order decay.** A more refined analysis (see Lemmas ?? & ??) shows:

$$|\partial_\theta \ell(\theta)| = \begin{cases} O(n\theta^{-8}), & \text{A1,} \\ O(n\theta^{-3}), & \text{A2.} \end{cases}$$

**4. Critical thresholds.** Set  $C_1 n\theta^{-8} = \varepsilon_{\text{grad}}$  for A1 and  $C_2 n\theta^{-3} = \varepsilon_{\text{grad}}$  for A2, then

$$\theta_{\text{crit}}^{\text{A1}} = \left( C_1 n / \varepsilon_{\text{grad}} \right)^{1/8}, \quad \theta_{\text{crit}}^{\text{A2}} = \left( C_2 n / \varepsilon_{\text{grad}} \right)^{1/3}.$$

With  $n = 1000$ ,  $\varepsilon_{\text{grad}} = 10^{-6}$ ,  $C_1 = 0.02$ ,  $C_2 = 0.002$ , one obtains  $\theta_{\text{crit}}^{\text{A1}} \approx 8.17$  and  $\theta_{\text{crit}}^{\text{A2}} \approx 126$ .

■

## D.4 Proof of Hessian Decay (Barrier 3)

**Theorem 4 (Hessian-Decay Behavior)** *Let*

$$\ell(\theta) = \sum_{i=1}^n \log c(u_i, v_i; \theta)$$

*be the log-likelihood for A1 or A2 copulas based on  $n$  data pairs. Then its second derivative (“scalar Hessian”) satisfies*

$$|\partial_\theta^2 \ell(\theta)| = \begin{cases} O(n\theta^{-9}), & \text{(A1),} \\ O(n\theta^{-4}), & \text{(A2).} \end{cases}$$

*Moreover, in double precision (machine epsilon  $\varepsilon_{\text{mach}} \approx 2.22 \times 10^{-16}$ ), the Hessian will underflow once*

$$n\theta^{-9} < \varepsilon_{\text{mach}} \implies \theta > (n/\varepsilon_{\text{mach}})^{1/9},$$

$$n\theta^{-4} < \varepsilon_{\text{mach}} \implies \theta > (n/\varepsilon_{\text{mach}})^{1/4}.$$

*For  $n = 1000$ , these evaluate roughly to  $\theta \gtrsim 1.2 \times 10^2$  for A1 and  $\theta \gtrsim 4.6 \times 10^4$  for A2.*

**Proof.** Let

$$\ell(\theta) = \sum_{i=1}^n \log c(u_i, v_i; \theta),$$

and write

$$D_i(\theta) = \partial_\theta \log c(u_i, v_i; \theta), \quad H_i(\theta) = \partial_\theta^2 \log c(u_i, v_i; \theta).$$

From Lemmas 1–2 we know

**1. A1 case:**

$$D_i(\theta) = C_i \theta^{-8} + R_i(\theta),$$

where  $C_i \neq 0$  is the leading constant and the remainder satisfies  $R_i(\theta) = O(\theta^{-9})$  as  $\theta \rightarrow \infty$ .

**2. A2 case:**

$$D_i(\theta) = D'_i \theta^{-3} + S_i(\theta),$$

with  $D'_i \neq 0$  and  $S_i(\theta) = O(\theta^{-4})$ .

Differentiate  $D_i(\theta)$  once more to get  $H_i(\theta)$ .

**A1:**

$$H_i(\theta) = \frac{d}{d\theta} (C_i \theta^{-8} + R_i(\theta)) = -8 C_i \theta^{-9} + R'_i(\theta),$$

and since  $R_i(\theta) = O(\theta^{-9})$ , we have  $R'_i(\theta) = O(\theta^{-10})$ . Hence

$$H_i(\theta) = O(\theta^{-9}).$$

**A2:**

$$H_i(\theta) = \frac{d}{d\theta} (D'_i \theta^{-3} + S_i(\theta)) = -3 D'_i \theta^{-4} + S'_i(\theta),$$

and  $S_i(\theta) = O(\theta^{-4})$  implies  $S'_i(\theta) = O(\theta^{-5})$ . Thus

$$H_i(\theta) = O(\theta^{-4}).$$

—

### Step 2: Sum over all $n$ observations

Since

$$\partial_\theta^2 \ell(\theta) = \sum_{i=1}^n H_i(\theta),$$

we get directly

**A1:**

$$\partial_\theta^2 \ell(\theta) = \sum_{i=1}^n O(\theta^{-9}) = O(n \theta^{-9}).$$

**A2:**

$$\partial_\theta^2 \ell(\theta) = \sum_{i=1}^n O(\theta^{-4}) = O(n \theta^{-4}).$$

### Step 3: Finite-precision underflow thresholds

In double precision, any quantity smaller in magnitude than  $\varepsilon_{\text{mach}} \approx 2.22 \times 10^{-16}$  will underflow to zero. Therefore solve:

**A1:**

$$n \theta^{-9} < \varepsilon_{\text{mach}} \implies \theta^9 > \frac{n}{\varepsilon_{\text{mach}}} \implies \theta > \left( \frac{n}{\varepsilon_{\text{mach}}} \right)^{1/9}.$$

For  $n = 1000$ , this gives  $\theta \gtrsim (10^3/2.2 \times 10^{-16})^{1/9} \approx 1.2 \times 10^2$ .

**A2:**

$$n \theta^{-4} < \varepsilon_{\text{mach}} \implies \theta^4 > \frac{n}{\varepsilon_{\text{mach}}} \implies \theta > \left( \frac{n}{\varepsilon_{\text{mach}}} \right)^{1/4}.$$

Numerically this is  $\theta \gtrsim (10^3/2.2 \times 10^{-16})^{1/4} \approx 4.6 \times 10^4$ .

These thresholds mark where the scalar Hessian effectively underflows, causing any Newton-type update to stall. ■